ICAS-88-6.8.1

THE APPLICATION AND IMPROVEMENT OF "WALL PRESSURE SIGNATURE" CORRECTION METHOD FOR THE TUNNEL WALL INTERFERENCE

Jiang Guiqing
China Aerodynamic Research and Development Center

Summary

The application and improvement of the "wall pressure signature" correction method developed by J.E.Hackett and the others is presented in this paper. The improvement of the method is characterized by higher accuracy of correction results and great reduction of the computing time for the real-time correction of test data by simplifying the algorithm. More than ten demonstration test results for the model pressure measurement and force measurement are presented here while some important problems concerning the correction for tunnel wall interference are analysed, demonstrated and computed.

Symbols

H height of test section
B width of test section
K ratio of test section height to width, $K=H/B$
S reference area of model
C cross-sectional area of test section
ε model blockage ratio, $\varepsilon=s/c$
BE model span relative to tunnel test section width
U_∞ velocity of free-stream
$\bar{Q}$ non-dimensional strength of line source, $\bar{Q}=Q/U_\infty C$
$\bar{\Gamma}$ non-dimensional strength of line vortex, $\bar{\Gamma}=\Gamma \cdot BE/U_\infty C$
M number of equivalent singularities
N number of wall-pressure measurement points at wall centreline of test section
C_D model drag coefficient
C_L model lift coefficient
Cm model pitching moment coefficient

Symbol Elements

$\Delta\bar{U}$ axial component of induced velocity, $\Delta\bar{U}=\Delta U/U_\infty$
$\Delta\bar{V}$ normal component of induced velocity, $\Delta\bar{V}=\Delta V/U_\infty$
W values at the centreline of side wall of test section
R values at the centreline of roof wall of test section
F values at the centreline of floor wall of test section
RF difference between values at a point at roof wall and its opposite point at floor wall
C values at tunnel centreline
Q values due to line source
G values due to line vortex
Cp pressure coefficient

Subscript

e values corresponding to effective position of model
k values corresponding to wing-and-body combination
T values corresponding to tail area
u uncorrected

1. Introduction

The classical "image" and "panel element" correction methods for the tunnel wall interference can not meet the requirements of data accuracy requested by some tests advanced in recent years, such as high angle-of-attack test, powered test and high lift test. Some progress in the study of wall interference correction has been achieved, and more than ten correction methods [1-5] by using wall pressure have been developed. Among them, the one developed by J.E.Hackett seems to be more mature for its convenience and economy, and correction accuracy. Some improvement to the method described in Ref.[1] has been made to further improve the correction computing time. As a result of using the method presented here, the

real-time correction during the test can be easily realized by microcomputer. Extensive demonstration tests have been conducted and the results are satisfactory.

2. Theorem and Improvement

To the "wall pressure signature" correction method, its unnecessary for us to describe and predict mathematically the tested model and its wake . The more necessity for it is to actually measure the signature of the wall interference—the wall pressure distributions, from which it is then possible to obtain the strength distribution of some simple line sources and vortices at fixed positions which induces the velocity distribution at the wall centreline of the test section equivalent to the velocity induced by the tested model. It is possible to use the wall interference of the line source and vortices to approach the wall interference for the tested model. Because such procedure does not relate to the actual flow around the tested model, the above-mentioned correction method is suitable to the wall interference correction of various models both for the lift effect and for blockage effect under various conditions.

In view of the error in the starting system of equations and its procedure block chart presented by the reference, it is necesscry to present equation system which determines the strength distribution of the line source Qi and vortex Γi simulating the model blockage effects and lift effects,

$$\sum_{i=1}^{MQ}\Delta\bar{U}WQ_{ji}\cdot\bar{Q}_i=\sqrt{1-\Delta C_{p,W_j}-\left(\sum_{i=1}^{MG}\Delta\bar{V}WG_{ji}\cdot\bar{\Gamma}i\right)^2}-1-\sum_{i=1}^{MG}\Delta\bar{U}WG_{ji}\cdot\bar{\Gamma}i$$

$$(j=1,2\cdots\cdots N) \qquad (1)$$

$$\sum_{i=1}^{MG}\Delta\bar{U}RFG_{ji}\cdot\bar{\Gamma}i=\sqrt{1-\Delta C_{p,R_j}}-\sqrt{1-\Delta C_{p,F_j}}-\sum_{i=1}^{MQ}\Delta\bar{U}RFQ_{ji}\cdot\bar{Q}_i$$

$$(j=1,2\cdots\cdots N) \qquad (2)$$

When it is difficult to distribute the wall pressure measurement points at the tunnel floor, Equ.(2) can be substituted with,

$$\sum_{i=1}^{MG}\Delta\bar{U}RG_{ji}\cdot\bar{\Gamma}i=\sqrt{1-\Delta C_{p,R_j}}-1-\sum_{i=1}^{MQ}\Delta\bar{U}RQ_{ji}\cdot\bar{Q}_i$$

$$(j=1,2\cdots\cdots N) \qquad (3)$$

The high-order terms are neglected in Equ.(1). It would be noted that the term "-1" at the right side of Equ.(1) and corresponding procedure block chart in Ref. [1] has been lost.

The wall pressure coefficient ΔC_p in the equation may be written as,

$$\Delta C_{p_j}=C_{p,\ model}-C_{p,\ no\ model} \qquad (4)$$

$\Delta\bar{U}WQ_{ji}$ is the axial non-dimensional veloity component induced by the i-th non-dimensional unit strength line soure and its wall effects at the j-th wall pressure measurement point at the side-wall centreline of the test section. The other symbols can be derived in the similar way. $\bar{Q}_i$ and $\bar{\Gamma}i$ are well distributed in the horizontal plane in which the model reference centre is located.

If the aerodynamic equivalent singularity has swept and angle-of-attack, $\Delta\bar{U}WG_{ji}$, $\Delta\bar{V}WG_{ji}$, and $\Delta\bar{U}RFQ_{ji}$ are not equal to zero, and $\bar{Q}_i$、$\bar{\Gamma}i$ can not be separated. In Ref. [1], the iterative process is adopted to obtain the solution. In this paper, a simplified algorithm is employed by approximately substituting the coupling effects of the blockage effects due to the model lift effects with a single horse-shoe vortex at the quarter-chord line. Firstly, $\bar{Q}_i$ distribution can be obtained from Equ.(1), then substitute it into Equ.(2) to obtain $\bar{\Gamma}i$. such solving process avoids a iteration and has been turned out to be a rather simple and convenient solution algorithm.

In general, the number of the wall pressure measurement points, N, is usually 4 to 5 times as many as the number of the aerodynamic singularities, M. Therefore, Equ.(1) and (2) is a contradictory linear equation system and it would be the most convenient apporach to use the "generalized inverse matrix method" to obtain the optimum opproximate solution, thus,

$$[\bar{Q}_i]=[\Delta\bar{U}WQ_{ji}]^+[\Delta\bar{C}_{p,W_j}] \qquad (5)$$

$$[\bar{\Gamma}i]=[\Delta\bar{U}RFG_{ji}]^+\{[\Delta\bar{C}_{p,RF_j}]-[\Delta\bar{U}RFQ_{ji}][\bar{Q}_i]\} \qquad (6)$$

and $$[a_{ji}]^+=\left([a_{ji}]^T[a_{ji}]\right)^{-1}[a_{ji}]^T \qquad (7)$$

$$\Delta\bar{C}_{p,W_j}=\sqrt{1-\Delta C_{p,W_j}-(\Delta VWG_{ji}\cdot\Gamma)^2}-1-\Delta\bar{U}WG_{ji}\cdot\bar{\Gamma} \qquad (8)$$

$$\Delta\bar{C}_{p,RF_j}=\sqrt{1-\Delta C_{p,R_j}}-\sqrt{1-\Delta C_{p,F_j}} \qquad (9)$$

$$\bar{\Gamma}=S.C_l u/2C \qquad (10)$$

$\Delta\bar{U}WG_j$ and $\Delta\bar{V}WG_j$ are the longitudinal and vertical non-dimensional velocity components at the j-th wall pressure measurement point of the side-wall centreline induced by the non-dimensional unit strength horseshoe vortex with swept and angle-of-attack and its wall effect at the quarter-chord line. For the given tunnel and given model, $[\Delta\bar{U}WQ_{ij}]^{+}$ "generalized inverse matrix" can be solved and stored into the computer beforehand for the use of real-time correction computing.

When the distribution of the aerodynamic equivalent singularities $\bar{Q}_i$ and $\bar{\Gamma}_i$ has been solved, using the wall influence coeficient matrix which has been solved and stored into the computer beforehand, the wall interference velocity distribution and hence the correction to the pressure measurement or the force measurement can be calculated.

· Correction to the Pressure Coefficient due to the Wall Blockage Interference

For the flow round a sphere, its correction formula of the pressure coefficients can be derived, as follows[10]:

$$C_p(x) = \frac{C_p u(x) - 1}{[1+\Delta\bar{U}CQ(X)]^2} + 1 \qquad (11)$$

In the case of small disturbance, the relation between disturbance velocity and pressure coefficient is:

$$\Delta C_p(x) = 2\Delta\bar{U}CQ(X) \qquad (12)$$

· Correction to Force and Moment Coefficients due to the Wall Blockage Interference

The wall blockage interference has two effects, one is to make the tested model actually placed in a flow field with higher speed than free stream speed; the other is to produce an extra translation acceleration in the model area. However, the correction to the drag coefficients due to the second effect as shown in Equ.(13) can be derived by applying momentum law in the axial direction.

$$\Delta C_D = -\frac{C}{S}[\Sigma\bar{Q}_i]^2 \qquad (13)$$

Defining the axial wall interference velocity as ΔUe, the correction to the drag coefficients due to the overall wall blackage interference may be written as:

$$C'_D = (C_{Dw} + \Delta C_D) / (1+\Delta\bar{U}e)^2 \qquad (14)$$

$$C'_L = K \cdot C_{Lw} \qquad (15)$$

$$C'_m = K\,(\Delta C_{mw} + (1+\Delta\bar{U}e)^2 \Delta C_{mw} / (1+\Delta\bar{U}_i)^2] \qquad (16)$$

where k is equal to C'_D/C_{Dw}, the supperscript " ' " refersto the value corrected for the wall blockage interference only.

As for the correction for the wall interference due to lift effect, it is similar to the traditional correction method, consequently, is unnecessary to be described in detail here.

3. Demonstration Model Tests

There're five examples of the demonstration, with two pressure measurement tests and three force measurement tests.

3.1 The pressure measurement tests were conducted in CARDC 1.4m×1.4m×2.8m low-speed wind tunnel with two sets of models, one set of blunt-nosed square cylinder models consisting of five models with same slenderness ratio of 3 and blockage ratios of 1.5%, 4.4%, 6%, 12%, 17.3% respectively and another set of streamline-nosed cylinder models with slenderness ratio 2.66 and blockage ratios of 4.4%, 6.0%, 12.0% and 17.5% respectively. All the data were obtained at the same Reynolds number. The corrected model pressure distribution and the wall pressure coefficients are shown in Fig.1 and Fig.2.

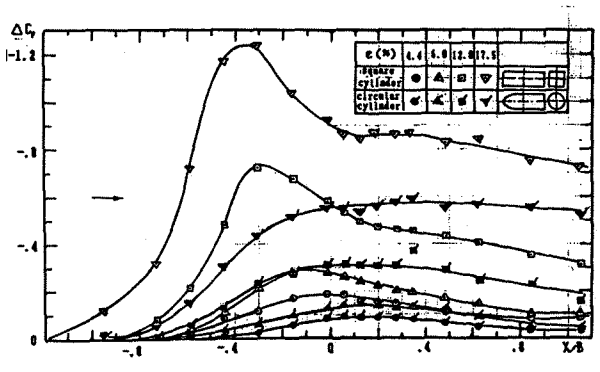

Fig.1. $\Delta C_p \sim X$ Curve
The Wall Pressure Distribution of the Cylinder Test

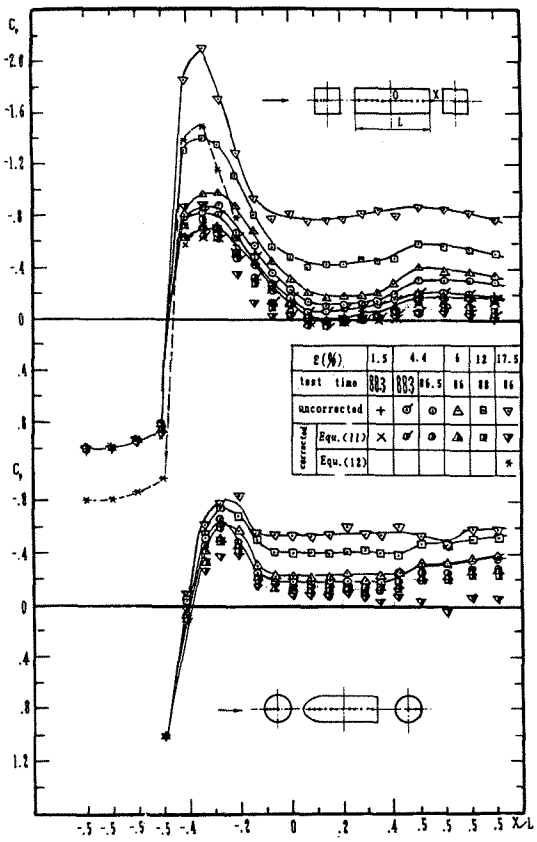

Fig. 2. Measured Pressure Distribution (uncorrected and Corrected) for the Cylinder Model.

3.2 Results for a half model of flat-plate wing with the aspect ratio (λ) of 3 and blockage ratio of 16.7% are shown in Fig.3, where the uncorrected data are from Ref. [2] and the wall interference-free data are reduced from the model tests with a set of blockage ratios of 1.5%, 6.3%, 9.8% and 16.7% presented in Ref. [2].

3.3 Results for wing-body combination obtained from the demonstration test, which was specially conducted with a set of models with blockage ratios of 6%, 9%, 12% and 15% respectively in CARDC 1.4m×1.4m tunnel at the same Reynolds number, are shown in Fig.4. The models tested consist of a circular cylinder fuselage with its diameter of 15% wing span and a straight flat-plate wing with aspect ratio of 4.

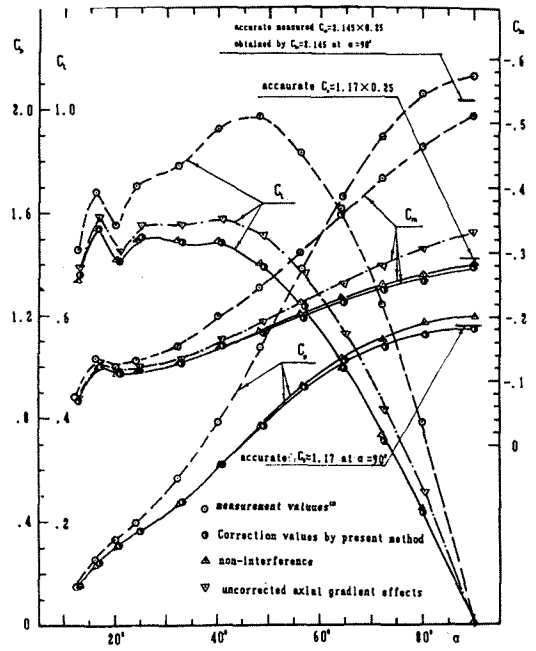

Fig. 3 The Comparison of the Flat-Plate Wing Correction Results

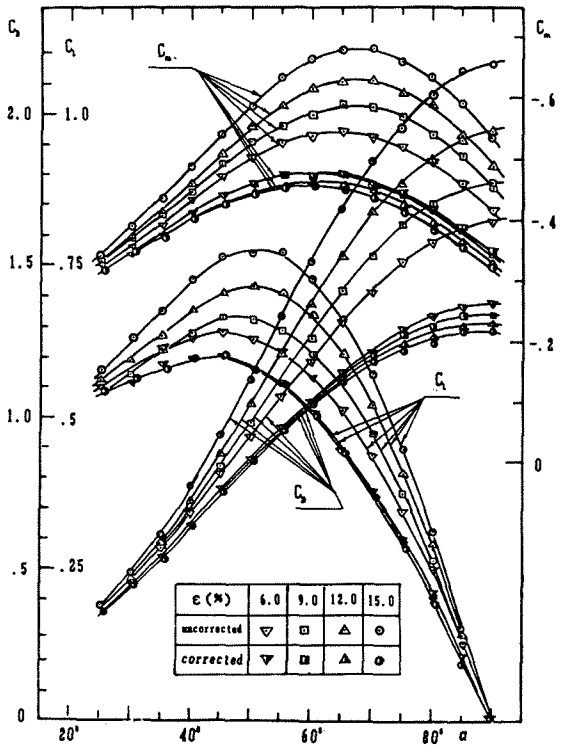

Fig. 4. The Correction Results for the Wing - Body Combination

3.4 Example 5 is the results for a wing-body-tail combination with applying span-wise blowing of the wing, which are also obtained from the test conducted in CARDC 1.4m×1.4m tunnel. The Wing of the model is of the trapezoidal one with a leading edge swept back of 44° and aspect ratio of 2.56. The slender ratio of the fuselage is 9.03 and the cross-section of body is a square with its four corners rounded off. The tail is of the trapezoidal one with a leading edge swept-back of 51.70. The exposed area of tail is 25% of the reference area of wing which accounnts for 11.8% of the cross-section area of test section. The span-wise blowing momentum coefficient Cμ is 0.06. The wall pressure distribution at the ceiling and floor of test section at typical angles of attack and the comparison of the correction results are given Fig.5 and Fig.6 respectively.

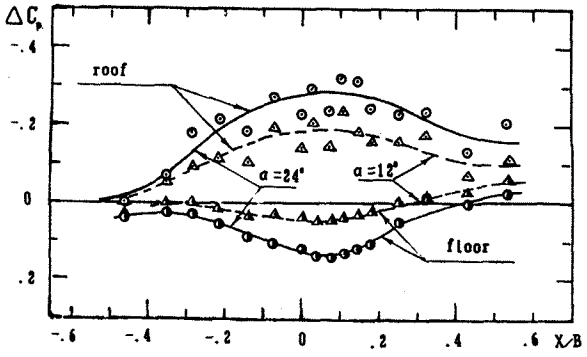

Fig.5. The Wall Pressure Distribution at the Ceiling and Floor of Test Section for the Span - Wise Blowing Model Test

4. Discussion

4.1 Figure.2 shows that no matter how big the blockage ratio of the tested model is , the tunnel wall doesn't interfere the pressure coefficients at the stationary points, which will not be demonstrated in detail here. However, the wall interference characteristics would be known physicaily according to the conservation of energy law. The wall interference would change the energy form in the flow field of test section, but wouldn't change the total energy of flow, namely, the total pressure between the far ahead of the model and its stationary poist remains unchanged or the pressure coefficient at the stationary point is always 1.0.

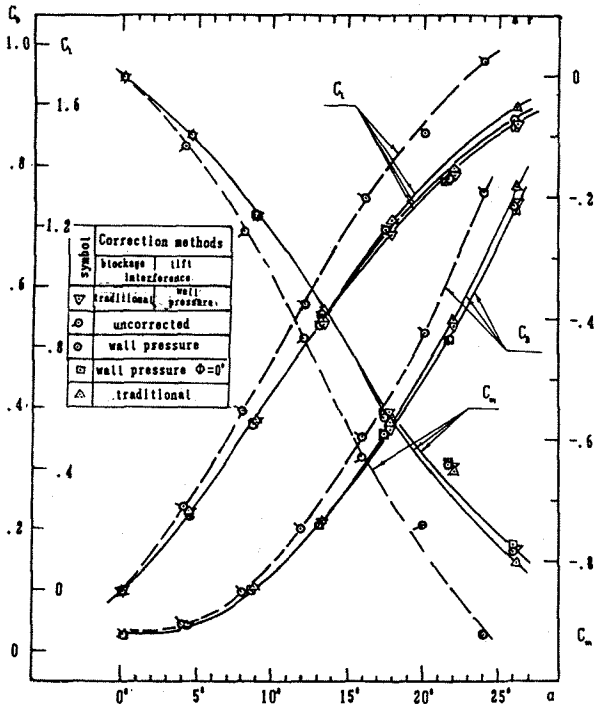

Fig.6 The Comparison of the Results from Different Correction Methods for the Span-Wise Blowing Model

For some reasons, the corrected results are not so good and hence the corrected results are scattered in some degree, but most of them are within the test error band. When the model blockage ratio is kept within 12%, its concordance is much better.

Figure.2 also shows clearly that Equ.(12), which is widely used in the wall interference correction, induces large errors to corrected results near the stationary points. It's easy to demonstrate that Equ.(12) is true only when both the wall interference and perturbance induced by the model satisfy the small disturbance condition, however, the model disturbance is always of the great one near the stationary points.

According to Equ.(11), the wall interference correction value of the pressure coefficients is always positive . As the measurement value approaches 1.0, the correction value reduces. When the measurement value is 1.0, its relative wall interferance correction value is 0. For the square cylinder with a blockage ratio of 17.5%, its pressure coefficient measurement value in the reattachment region is approximately -0.6, while correcting for the wall interference, it apporximalaly becomes 0 and is essentially the same as the

interference-free value. If the pressure coefficient is positive, the corrected pressure coefficients are higher than the uncorrected ones. If the measured coefficient is different and, even at the same axial position, wall interference correction value, no matter whe ther it's an absolute value or it's a relative value, is different.

Because of the above-mentioned wall interference law in the model pressure distribution, various correction methods which are used today for the wall blockage interference correction to the pressure measurement tests are unreasonable.

4.2 The computation sloving the singularity streagth distribution $\widehat{Qi}$ and $\overline{\Gamma}i$ is simplified in this paper. Because of avoiding the iteration and using the "generalized inverse matrix" method, various generalized inverse matrices and the matrices influencing coefficients for the specific tunnel and tested model can be calculated and stored into the computer before test in order to be used during real-time correction computing, consequently, the work load of real-time correction computing is little. The time needed for correcting a group of data at an attitude angle condition in Intel 86/330 microcomputer (approx. 20000～30000/sec.)is only one second, less than 1/100 of that needed for the program in Ref. [8], which was based on the method of Ref. [1].

4.3 It's known that in the traditional correction methods including Ref. [1, 2] only the "buoyant drag" correction to the drag coefficients is made for taking account for the extra translation acceleration effects due to the wall blockage interference in the model region. Fig.3 obviously shows that the correction results provided by the classical correction method are not accurate except the drag while that provided by the improved correction method given in this paper seems to be rather satisfactory.

Reference. [9] presents the comparison between results for the two-dimensional flat-plate with blockage ratios of 35.5% and 9% at high angle-of-attack up to 90°. For the flat plate with a blockage ratio of 35.5%, the wall interference value at high angle-of-attack is approximately two times of truth value, and its effects of the wall interference due to the translation acceleration effect amount to more than 25%. Although the interference-free results are not given in Ref. [9], the following equation at high angle-of-attack is presented,

$$(C_{0}35.5\%-C_{0}9\%)\ /C_{0}9\%=(C_{l}35.5\%-C_{l}9\%)\ /C_{l}9\% \qquad (17)$$

This provides another evidence which confirms the improvement to the correction method made by the author.

4.4 Figure.4 shows that the wall interference correction for the set of wing-body combination test results is not so satisfactory and three aerodynamic coefficients are over-corrected, but the law seems to be essentially the same with that of the corrected relative values. This proves again that the correction method for the gradient effects in this paper is reasonable. The reasons for over-correcting is that the downstream measurement points on the wall are not far enough and the apporaching value, i.e. the value which doesn't vary with the distance from the model, could not be obtained due to the large demension of model relative to the test section when half model is used for the test. That has been shown by the curve of the wall pressure distribution and the further analytical computation (see Tab.1.).

Tab.1 The Effect of Wall Pressure Measurement Rang on the Correction by Present Method

model	angle of attack α	measurement values (C_{m})	correction values bg present method (C_{m})		
			$\overline{X}\leq 1.0$	$\overline{X}\leq 0.60$	$\overline{X}\leq 0.43$
flat-plate wing ε=16.7%	72.41°	1.909	1.088	0.993	
	80.24°	2.078	1.133	0.989	
	90°	2.145	1.159	0.882	
wing-body combination ε=15%	75.26°	1.965	1.220	1.053	0.994
	80.17°	2.063	1.242	1.044	0.991
	85.08°	2.140	1.282	1.065	0.984
	90°	2.160	1.285	1.037	0.951

Remarks,

1. the model center is at X=0; 2. the trends for the other aerodynamic components are the same as for C_D.

It would be noted from Tab.1 that the wall interference correction values might be excessively great once the tunnel test section is too short or the model is installed far-downstream. This is mainly caused from the overestimation of $\Sigma\overline{Q_i}$ value, consequently, the effects on the wall interference corection for the pressure measurement are unremarkable.

4.5 The example shown in Fig.6 is served to compare the correction results obtained by the conventional correction method and the "wall pressure signature" correction method at low to medium angles of attack. Though the wall pressure distribution at the ceiling is somewhat dispersive (seen in Fig.5), the correction results are not influenced remarkably (seen in Fig.6). Fig.6 shows that within $\alpha \leqslant 15°$, no appreciable differences between the corrected results given by different methods can be observed, though the differences increase with the increasing of angle of attack. This is a calibration model test and the corrected results provided by the "wall pressure signature" correction method are much more accurate than those given by other methods.

Within the test angle-of-attack range of this example, the effects of the swept-back are little, but at high angles-of-attack, especially at high lift, the effects of the swept-back, i.e the coupling effects of the blockage and the lift effects, may become serious, as shown in Tab.2.

During the test at high angles-of-attack and high lift, the wall interference would be over-corrected once the swept coupling effects haven't been included.

5. Conclusions

5.1 The time needed for real-time correction computing is reduced greatly due to the simplification to the correction method developed by the author and the using of "generalized inverse matrix method". The real-time correction of the test data can easily be realized by even a microcomputer.

5.2 For all aerodynamic coefficients, besides the drag coefficients, the axial gradient effects due to the wall blockage interference have to be corrected. The present method is not only simple and convenient, but also accurate.

5.3 For the pressure measurement test, the traditional correction methods being used today are uncorrect. Equ.(12) is not excellent while Equ.(11) is universely suitable.

5.4 The wall produces no interference to the pressure at stationary points of the model and the measured pressure coefficients at the stationary points is always 1.0.

Tab.2 Influence of Swept Effects on Correction

C_{D_u}	aerodynamic coefficients	measurement values	correction values by present method	
			swept effects included	no swept effects included
0.98	C_L	0.980	0.697	0.679
	C_D	1.087	0.773	0.753
	C_m	-.2448	-.1741	-.1695
2.00	C_L	2.00	1.471	1.385
	C_D	1.087	.799	0.753
	C_m	-.2448	-.1800	-.1695

Remarks,

1. α=48°, ε=16.7%, $\Phi_{1/4}$=50°; 2. without correction for wall lift effects; 3. identical pressure distribution is used in both corrections with and without swept effects.

5.5 The wall pressure distribution behind the model has to be downstream enough, otherwise the wall interference to the force and moment coefficients would be over-corrected. However, the influence on the correction results for the pressure coefficients is unremarkable.

5.6 In general, for the high swept-back model, the coupling effects can not be included over the range medium angles of attack, but have to be included at high angle-of-attack and high lift otherwise the correction values would be excessively great.

Reference

1. Hackett, J.E. Sampath, S.S. and Phillips, C.G., "Determination of Wind Tunnel Constraint Effects by a Unified Pressure Signature Method, Part I, Applications to Winged Configurations", NASA CR 166186, 1981.

2. Hackeff.J.E., Wilshder, D.J.and Lilley, D.E., "Estimation of Tunnel Blockage from Wall Pressure Signatures, A Review and Data Correction", NASA CR 152241. March 1979.

3. Moses, D.F., "Wind Tunnel Wall Correction Deduced by Iterating from Measured Wall Static Pressure", AIAA Journal Dec. 1983.

4. Zhou Changhai, "The Integral Method of Correction for the Low Speed Wall Interference", Aerodynamic Research and Experiment, June 1985.

5. You peichu, "Computation of the Wall *Interference Correction in the Airfoil Test by the* Wall Pressure Measurement", Northwest polytechnical University, 1985.

6. Ashill, P.R. and Weeks, D.J., "A Method for Determing Wall Interference Corrections in Solid-Wall Tunnel from Measurements of Static Pressure at the Walls", AGARD CP 335.

7. Rizk, M.H. and Smithmeyer, M.G., "Wind-Tunnel Wall Interference Corrections for Three-Dimensional Flow", Journal of Aircraft Vol.19, Jane 1982.

8. Chen Mingyan, "Computation of Wall Interference of High Angle-of-Attack by Measurements of static Pressure at the Walls", Nanjing Institute of Aeronautics and Astronautics, Aug.1985.

9. Modi, V.J. and EL-Sherbiny, S., "Wall Confinement Effects on Bluff Bodies in Turbulent Flows", Proc. 4th Int. conf. Wind Effects on Buildings and Structures, England, 1975, PP. 121-130.